

A Tail-Worn Sensor-Equipped Heart Rate Measurement Apparatus for Ischemic Stroke Prevention

Chi-Chun Chen^{1,†}, Ching-Ping Chang²

Abstract

Objective:

This paper presents a tail-worn sensor-equipped heart rate measurement apparatus to quantify the effect of exercise preconditioning on the physical disability of rats due to ischemic stroke. So far, physiological measurements in the literature are mostly conducted in an invasive manner, meaning that sensor implant surgery is a necessity, and result in the risk of infection and the problem of interrupted data capture. Nonetheless, most existing non-invasive physiological measurement apparatus are designed for animals at rest, not on the move. For this sake, this heart rate measurement apparatus was developed as an easy-to-use, but high performance, non-invasive tool for long-term physiological monitoring on rats, particularly in the running state.

Methods:

The presented non-invasive measurement apparatus comprises a front-end PPG sensor array and a back-end digital signal processor. A PPG signal was chosen for back-end signal extraction, using an adaptive filter and Hilbert-Huang Transform (HHT). This work was experimentally validated by the heart rate variability due to the epinephrine administration to rats in the conscious and unconscious states, and a heart rate monitoring in the running state was performed at the end of this work.

Results:

Rats under test were equally divided into two groups for comparison purposes, one as the control group and the other as the exercise group, and each member in the latter needs to take a 3-week physical training program as a preconditioning. In weeks 1–3, the exercise (control) group members demonstrated an average pre-exercise heart rate of 358.31 (356.89), 328.21 (360.1) and 312.91 (361.68) BPM, respectively. The exercise group members clearly have a much slower pre-exercise average heart rate than the control group in weeks 2–3, indicating a negative correlation between the heart rate and the slide angle result of an inclined plane test.

Conclusions:

This paper presents a novel physiological measurement apparatus as a non-invasive alternative to a typical inclined plane test for quantifying the benefit of exercise preconditioning to ischemic stroke prevention. Featuring low physical confinement on animals and long-term monitoring, it was experimentally validated herein as an easy-to-use, but high performance, tool, and is expected to be employed in futuristic clinical research.

Keywords

Tail-worn, Sensor-equipped, Hilbert-Huang transform (HHT), Heart rate, Inclined plane test

¹Department of Electronic Engineering, National Chin-Yi University of Technology, Taichung, Taiwan

²Department of Medical Research, ChiMei Medical Center, Tainan, Taiwan

[†]Author for correspondence: Chi-Chun Chen, Department of Electronic Engineering, National Chin-Yi University of Technology, Taiwan, Tel: +886-4-23924505-7316; Fax: +886-4-23926610; email: chichun@ncut.edu.tw

Introduction

The benefit of exercise has long been well validated in the literature, e.g. cardiovascular disease prevention [1-2], brain ischemic tolerance improvement [3-4], and more. However, physical impairment due to excessive exercise had been reported as well, such as muscle cramps [5], osteoarthritis [6], rhabdomyolysis [7,8], serious renal injuries [9] and sudden cardiac death [10]. Hence, benefit of exercise to illness prevention has long been an issue of great interest in physiology and related disciplines, but in the absence of an easy-to-use, but high performance, tool for physiological monitoring, say, heart rate variability during exercise.

So far, animal tests for exercise effect investigation are often conducted on rodents, e.g. rats [11-14]. Today, treadmills and running wheels are the most common animal test beds to observe the benefit of physical training. As in [11,14,15], animals under test were trained at a constant running speed for a specified duration, as an exercise preconditioning for subsequent study on ischemic stroke effect. The preconditioning can be classified as effective and ineffective, and was defined as the incidents when a rat stumbles, falls and even grabs the rail once unable to catch up with the running wheel speed [16-18]. Needless to say, incidents of ineffective exercise significantly reduce the exercise benefit, and it was validated to be correlated with the brain infarction volume using an IR sensor-equipped running wheel [17]. Up to now, physiological signals are measured in an invasive and a non-invasive manner. In the former case, sensors must be embedded into animals by surgery in advance, which cannot be performed on tiny mice [19-22], resulting in an increase in the experiment complexity, and rats have the risk of infection as a consequence [23]. Even though invasive measurement apparatus were designed to monitor the physiological conditions of rats in either anesthetized or conscious state with a low physical confinement feature [22], a major disadvantage is the battery capacity limit of a battery powered wireless transmission module, that is, a long-term monitoring is non-feasible. Consequently, non-invasive physiological measurements were conducted in two ways. In the first way, measurements were performed on restrained and conscious rats [24-25], while, in the second way, body-worn sensors were employed to eliminate the above-stated physical restraint [23]. However, it is rather difficult to place a sensor precisely onto a specific spot of a

rat's body. Particularly, rats must be physically confined to some extent for successful data sensing, meaning that physiological monitoring cannot be performed on rats in the running state. Though there have been a wide variety of animal physiological measurement apparatus, the integration of a measurement apparatus into an animal test bed remains hardly addressed, presumably due to the difficulty in motion artifact removal.

Motion artifact refers to a collective signal disturbance resulting from the relative movement between a creature under test and the sensors attached thereto, and have long been a key challenging issue in exercise physiology. As the worst case, physiological signals may be completely overridden. In this work, measurements were conducted on not well-controlled rats, meaning that it is definitely a non-trivial task to remove the unwanted motion artifact. In an attempt to extract the signal of interest, motion artifact was removed herein using a combination of PPG signal capturing in the front end and a non-stationary signal processor in the back end. Once validated, this work is expected to be widely applied to the studies in physiology and related fields.

This paper aims to integrate a running wheel-based test bed and a mechanism to quantify the benefit of exercise to ischemic stroke prevention, and is expected to be applied to further studies in relevant disciplines in the future. This innovation provides a more convincing analysis on physiological conditions, due to non-invasive measurements and a low physical confinement imposed on rats.

Methods

As a three-stage approach, this work is outlined as follows. In Stage 1, a non-invasive physiological measurement apparatus is developed with photoplethysmogram (PPG) and a triaxial accelerometer as a front-end sensor set, and a front-end circuit is designed as well to acquire PPG signal. Subsequently, the signals acquired in stage 1 are processed in Stage 2. This is done by firstly removing the motion effect using the feedback signals of the triaxial accelerometer as a reference, and then the desired PPG signal of a rat in motion can be effectively extracted by taking Hilbert-Huang transform (HHT). Finally, Stage 3 is designed to validate the performance of this apparatus in four states, i.e. the anesthetized, restrained, freely moving and running states.

■ Non-invasive physiological measurement apparatus

As explicitly stated previously, Stage 1 aims to develop a non-invasive physiological measurement apparatus. As illustrated in **Figure 1**, the left half involves a PPG array circuit, formed by 3 independent PPG extraction circuits, and a triaxial accelerometer circuit, and can be powered by a 9 V battery, or plugged into AC power sources through an adapter. Through respective voltage regulators, the power supply powers the PPG array circuit, the triaxial accelerometer extraction circuit and an ARM-based microcontroller unit (MCU). Extracted signals can be simply stored in an SD card, or transmitted to a PC via an USB to UART bridge for subsequent signal processing.

■ PPG extraction circuit

Periodic variation in blood concentration and PPG signals are sensed using a reflective optical sensor TCRT1000, consisting of an IR emitter and an IR phototransistor. This is done by means of the intensity of the reflected IR signals from the tail of a rat. The PPG sensors can be placed anywhere due to the fact that there are plenty of micro blood vessels and four major vessels over the tail, meaning that the ECG sensor alignment problem suffered in a conventional body worn device can be completely resolved [23]. As illustrated in **Figure 1**, a PPG array circuit, composed of three independent extraction circuits, is employed herein to measure PPG signals at various locations followed by corresponding INA333 instrumental amplifiers. As expected, PPG signals are accompanied by DC offset, breath, body jitters, 60 Hz signal and higher frequency components, all of which are treated as noise and can be filtered out using a 2nd order low pass Butterworth filter with a cutoff frequency of 20 Hz. As illustrated in **Figure 2**, the filtered PPG signals are then applied to a cascade of 3 amplifiers with a gain of 10 for subsequent motion artifact removal. The output signal of each stage is then converted into digital form using an ADS8344 ADC.

■ Triaxial accelerometer extraction circuit

As illustrated in **Figure 3**, an LIS344ALH 3-axis accelerometer is employed as the front-end sensor, and the acceleration signals along the x, y and z axes are applied to respectively voltage followers to avoid loading effect. The output analogue signals are then converted to digital forms using an ADS8344 ADC, as in **Figure 3**.

■ PPG signal extraction

In Stage 2, signal processing is performed on the raw PPG signals of a rat in motion. The unwanted motion artifact effect can be removed to a certain extent using the output signal of the ADS8344 in **Figure 3** as a reference, after which desirable PPG signals can be extracted using Hilbert-Huang transform (HHT).

■ PPG signal processing

Motion artifact has long been an issue of interest and great concern in the literature, simply for the reason that it significantly interferes with the desired physiological signals. Using a PPG sensor array, raw signals are measured at 3 positions, each of which is then amplified 10, 100 and 1000-fold, as a way to prevent signal saturation due to over amplification. Moreover, the output signals of a triaxial accelerometer were employed as a reference in an attempt to remove a motion artifact. As illustrated in **Figure 4**, this study is presented as a two-stage mechanism. Stage 1 is designed to remove motion artifact using an adaptive filter. A raw signal, decomposed into a desired PPG signal and the noise n_o , is applied to an input of the adaptive filter, and the noise n_i , correlated with n_o but uncorrelated with S , is applied to the other input. n_i is simply the above-stated reference to remove the motion artifact, and the output Y can be found using the transfer function H . The desired PPG signal is approximated as the output $Z = S + n_o - n_i$. In theory, there is no way that n_o can be completely removed using a time-invariant filter, since the motion artifact is time-dependent, meaning that the filter must be made adaptive, using the output Z as a feedback signal for H . As illustrated, the output signal Z , sorted into poor and good signals according to the level of motion artifact, is further processed in Stage 2 for accurate signal extraction. Poor and good signals are processed using HHT and a zero-phase digital filter, respectively.

Post-end signal processing is performed using HHT [26], since the measured PPG signals would be very likely either unsteady or non-linear. HHT is an empirical way of signal processing, and has been widely and successfully applied to signal extractions in health care issues, e.g. heart rate variability [27] and blood pressure measurement [28]. HHT was developed as a 2-stage approach. In stage 1, a piece of data is decomposed into a number of intrinsic mode functions (IMFs), using the empirical decomposition (EMD) technique. In stage 2,

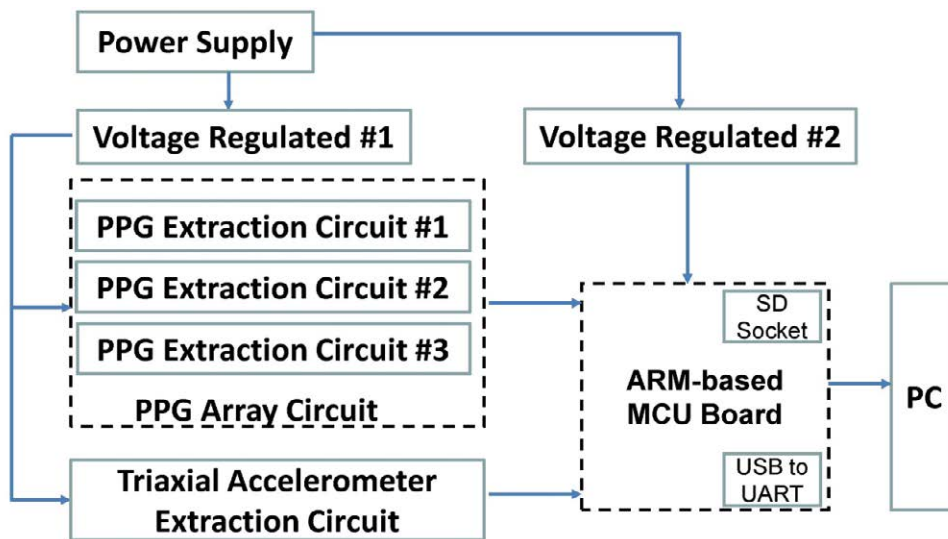


Figure 1: Front-end signal sensing and delivery.

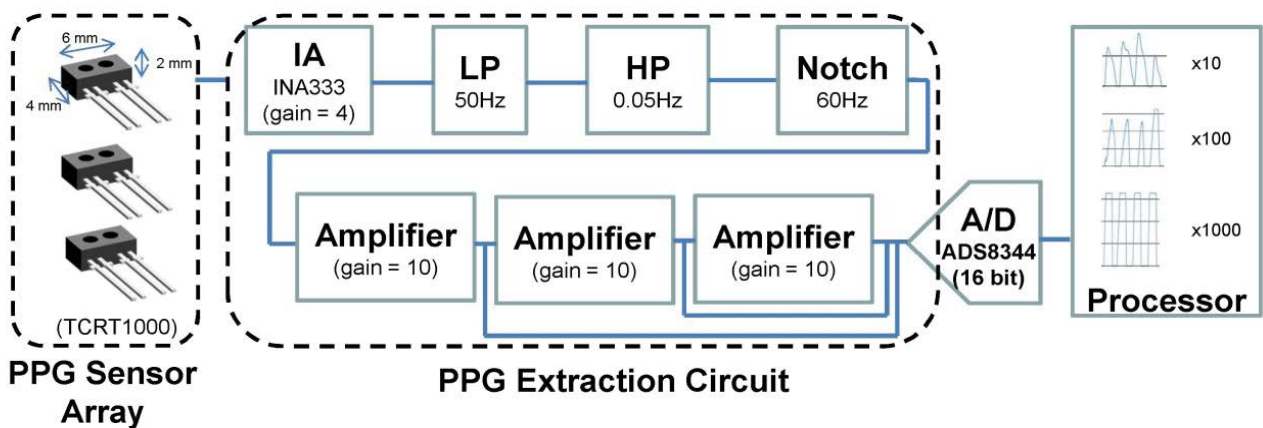


Figure 2: A three-stage cascade amplifier for PPG signal amplification.

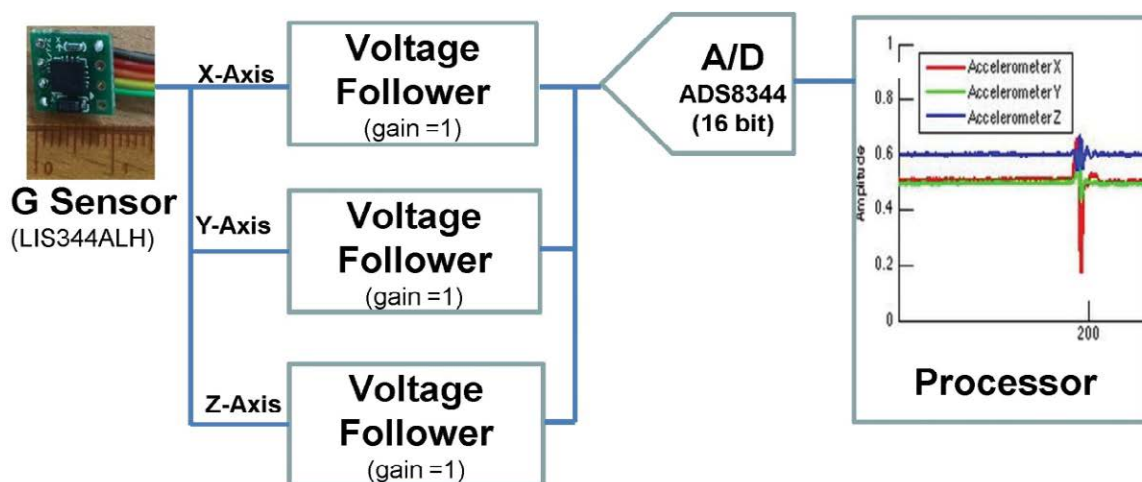


Figure 3: Acceleration signal capturing using a G sensor.

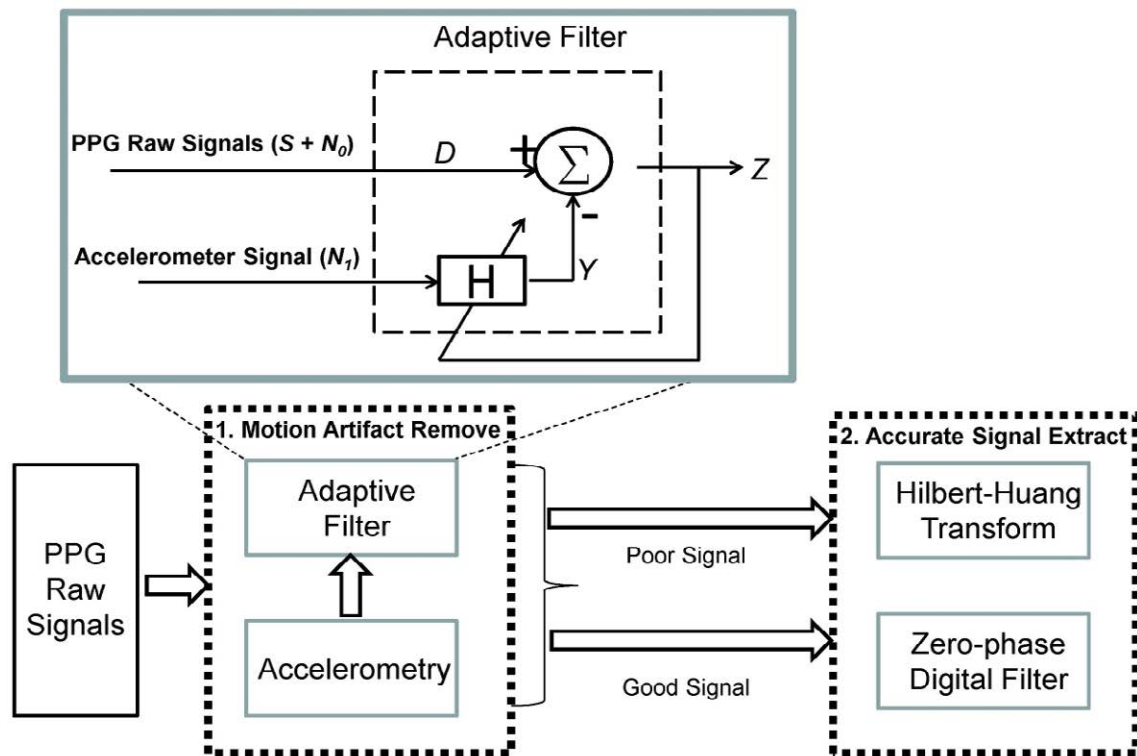


Figure 4: Back-end PPG signal processing.

signal extraction is performed on the IMFs using HHT. As illustrated in **Figure 5**, Steps 1–6 are repeated to find IMFs until a monotonic function $r_n(t)$ is seen. For instance, $IMF(b_1) = X(t) - m_1$ represents the first component, where $X(t)$ and m_1 symbolize an original signal and the envelope of the mean value, respectively, etc. Energy–frequency–time distributions of all the IMFs are then revealed using HHT.

■ **Performance validation**

In this work, three-stage performance validation is performed in the anesthetized, restrained, freely moving and running states, as illustrated in **Figure 6**. Excluding the anesthetized case, rats are all tested in conscious state. Steady heart rate is measured in the first validation stage. In contrast, a heart rate comparison is made in the anesthetized, restrained and freely moving states before and after using Epinephrine. In the first two validation stages and in the anesthetized state, performance is compared with a BIOPAC MP150 data acquisition system. In the final validation stage, motion artifact is firstly removed in an effective manner using an adaptive filter, and the heart rate signals of interest in running state are then accurately extracted from raw PPG signals using HHT.

■ **Heart rate measurement in the anesthetized state**

As a preliminary step to conduct experiments, a rat was anesthetized using (1–2 g/kg, i.p. Sigma, China). Once the rat was in the anesthetized state, a PPG sensor array was attached to its tail for subsequent measurement. Illustrated in **Figure 7(a)** are the raw data taken at the outputs of cascaded amplifiers, **Figure 7(b)** are a bandpass filtered signal between 3 and 15 Hz of the output signal of the second stage and the spectrum thereof giving a dominant frequency at 5.4 Hz, i.e. the heart rate signal of interest, **Figure 7(c)** are the detected peaks and the RRI histogram of the first 100 pieces of data, and **Figure 7(d)** is the HRV spectrum of the RRI in **7(c)**.

Meanwhile, the physiological signal measurement was conducted using a BIOPAC MP150 data acquisition system for comparison purposes. BIOPAC MP150 uses a physiological amplifier, taking signal form a femoral artery, to monitors physiological conditions. A BIOPAC MP150 operates at a sampling rate of 1 KHz, while the presented apparatus works at 100 Hz. For this sake, the PPG data sampled by the BIOPAC MP150 must be resampled for a linear regression

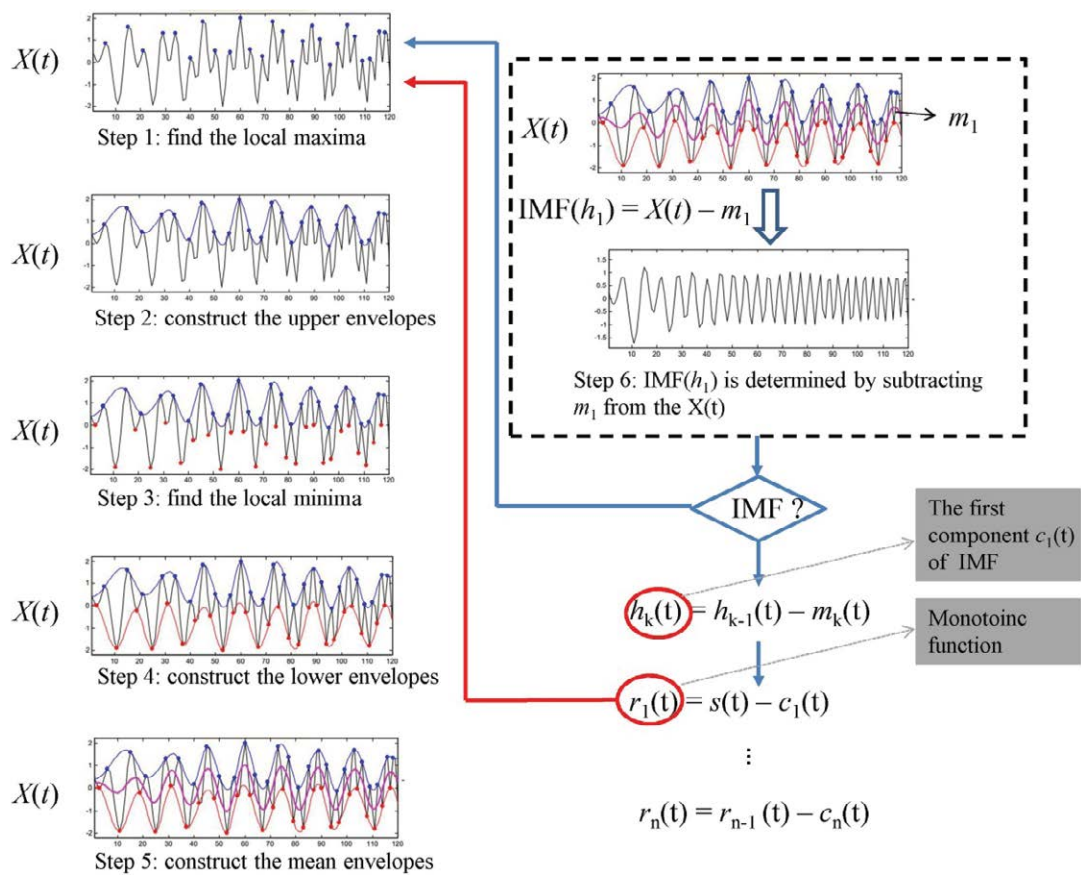


Figure 5: An illustration of empirical mode decomposition.

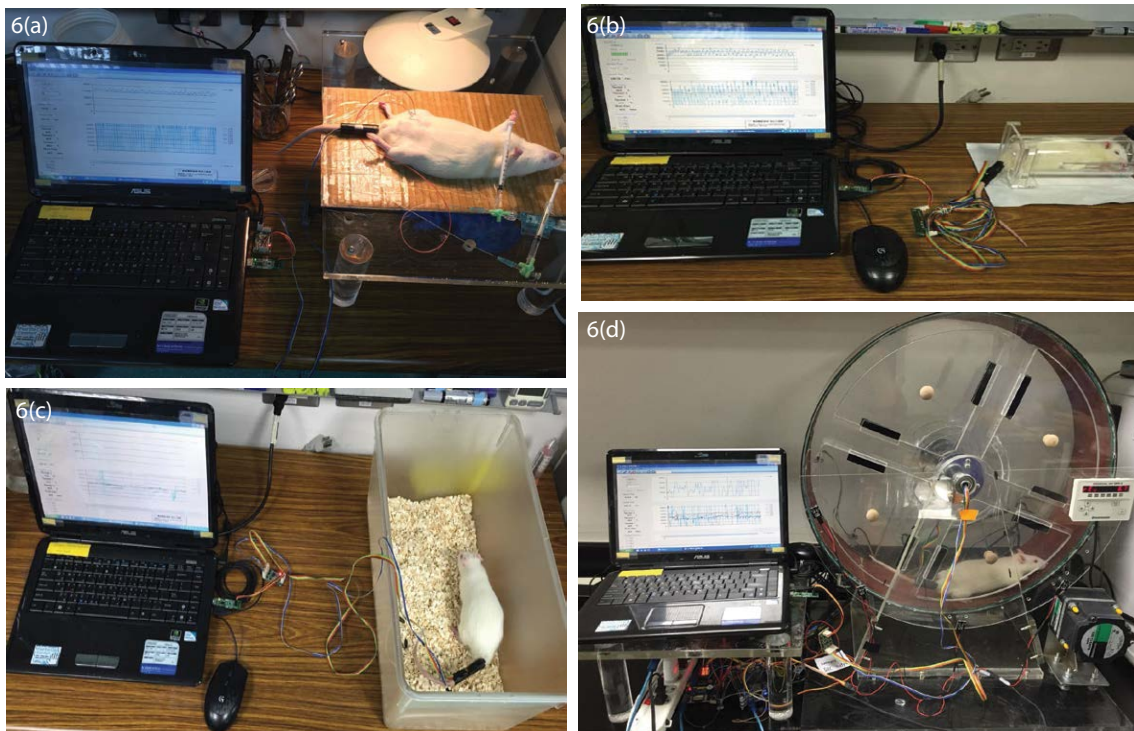


Figure 6: Heart rate measurement for a rat in the (a) anesthetized, (b) restrained, (c) freely moving and (d) running states.

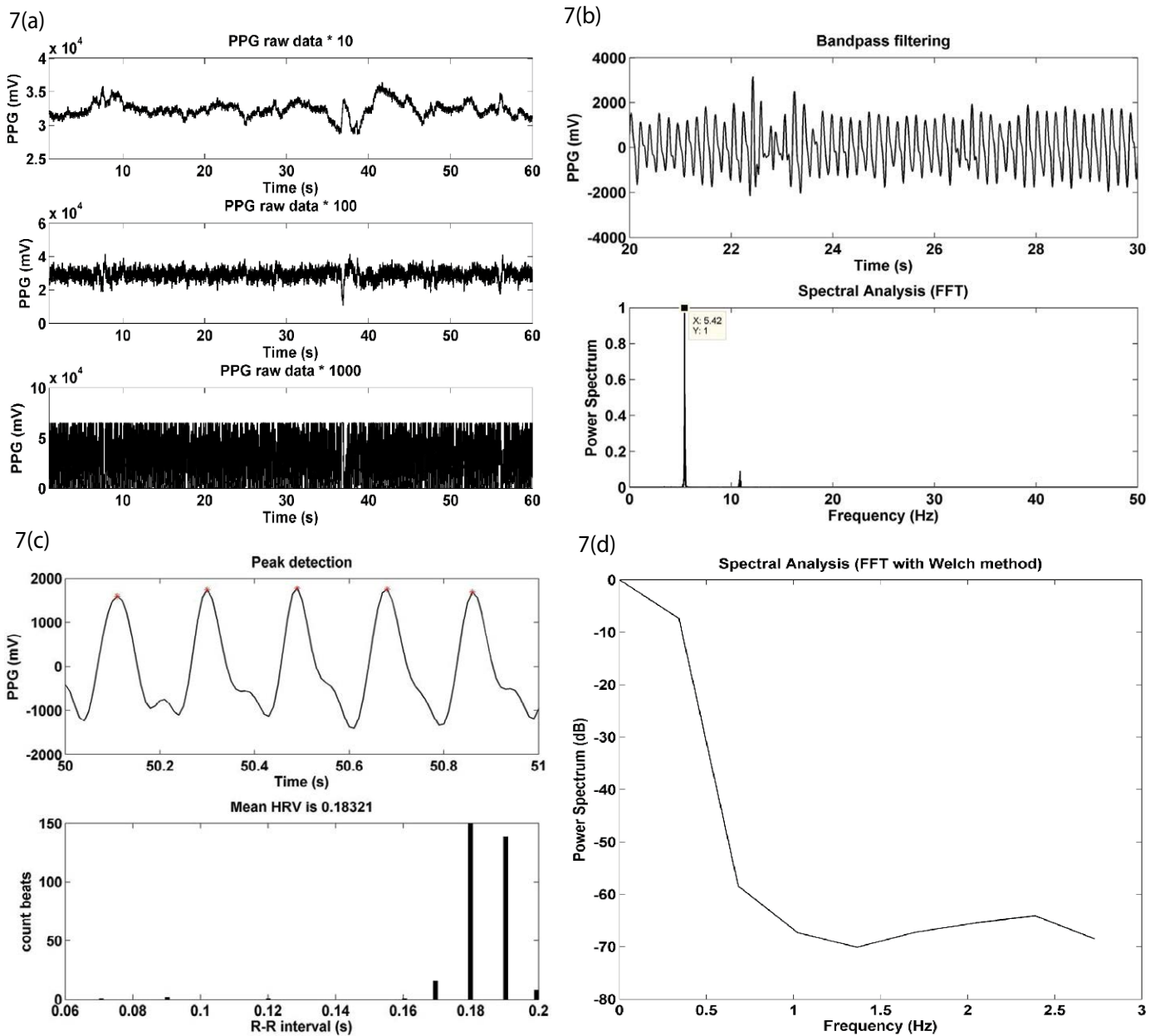


Figure 7: Experimental results in the anesthetized state.

analysis. There is a correlation up to 0.97 in the anesthetized state.

■ **Test on varying heart rate**

Epinephrine is known to speed up the heart rate of the mammals, and is treated as a way to validate the performance of this work. Illustrated in **Figure 8(a)** are the raw PPG signals at respective stages, and effect of Epinephrine is significantly reflected by the first stage output signal during the Epinephrine injection, while is accompanied by signal saturation at the second and the

third stage due to over amplification, until the effect is gone. The high signal fluctuation may be ascribed to the pressurized blood vessels during the Epinephrine injection. **Figure 8(b)** gives a bandpass filtered signal of the raw data in **Figure 8(a)** and a power spectrum with a dominant frequency. A comparison on the detected peaks before and after the use of Epinephrine is illustrated in **Figure 8(c)**, where there are a clear rise in the heart rate and an average RRI of 0.16. In a comparison with **Figure 7(d)**, there is a minor increase over low frequency components in **Figure 8(d)**.

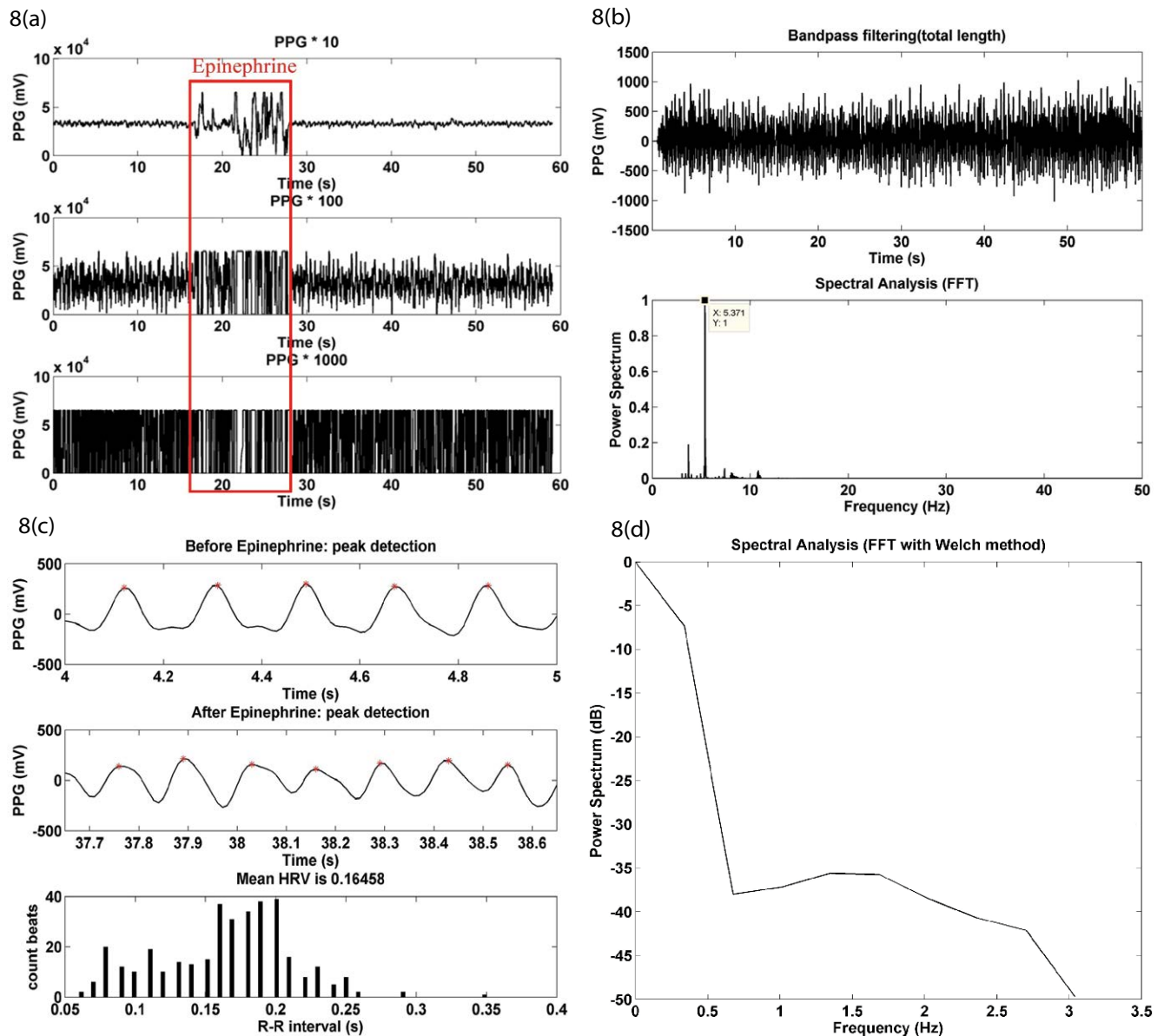


Figure 8: Experimental results before and after the use of epinephrine in the anesthetized state.

As illustrated in **Figure 6(b)**, the restrained state refers to a state in which a rat under test is physically and tightly confined within a small acrylic case, but remains in conscious state. As in the anesthetized state, epinephrine is used to speed up the heart rate for the performance validation of this work. Just as in **Figure 9(a)**, there are a tremendous signal variation in the first stage and signal saturation in the second and the third stages of the cascade amplifier. Bandpass filtering of the raw PPG signal in **Figure 9(a)** clearly gives a dominant frequency in **Figure 9(b)**. **Figure 9(c)** gives a detected peak comparison before and after the use of Epinephrine, reveals a rise in the heart rate, and

indicates an average RRI of 0.13. In comparison with **Figure 7(d)**, there is a minor upward shift over low frequency components in **Figure 9(d)**.

In the freely moving state, the PPG sensor array was first attached to the rat's tail, and the rat was placed in an uncovered box for observation, as illustrated in **Figure 6(c)**. The rat was taken out of the box, and the upper part of the body, including the head, was wrapped using a piece of opaque fabric for the injection of epinephrine. The rat was replaced into the box right after the injection. **Figure 10(a)** gives the waveforms of the raw PPG signals of the three stage cascade amplifier, and signals varied significantly and

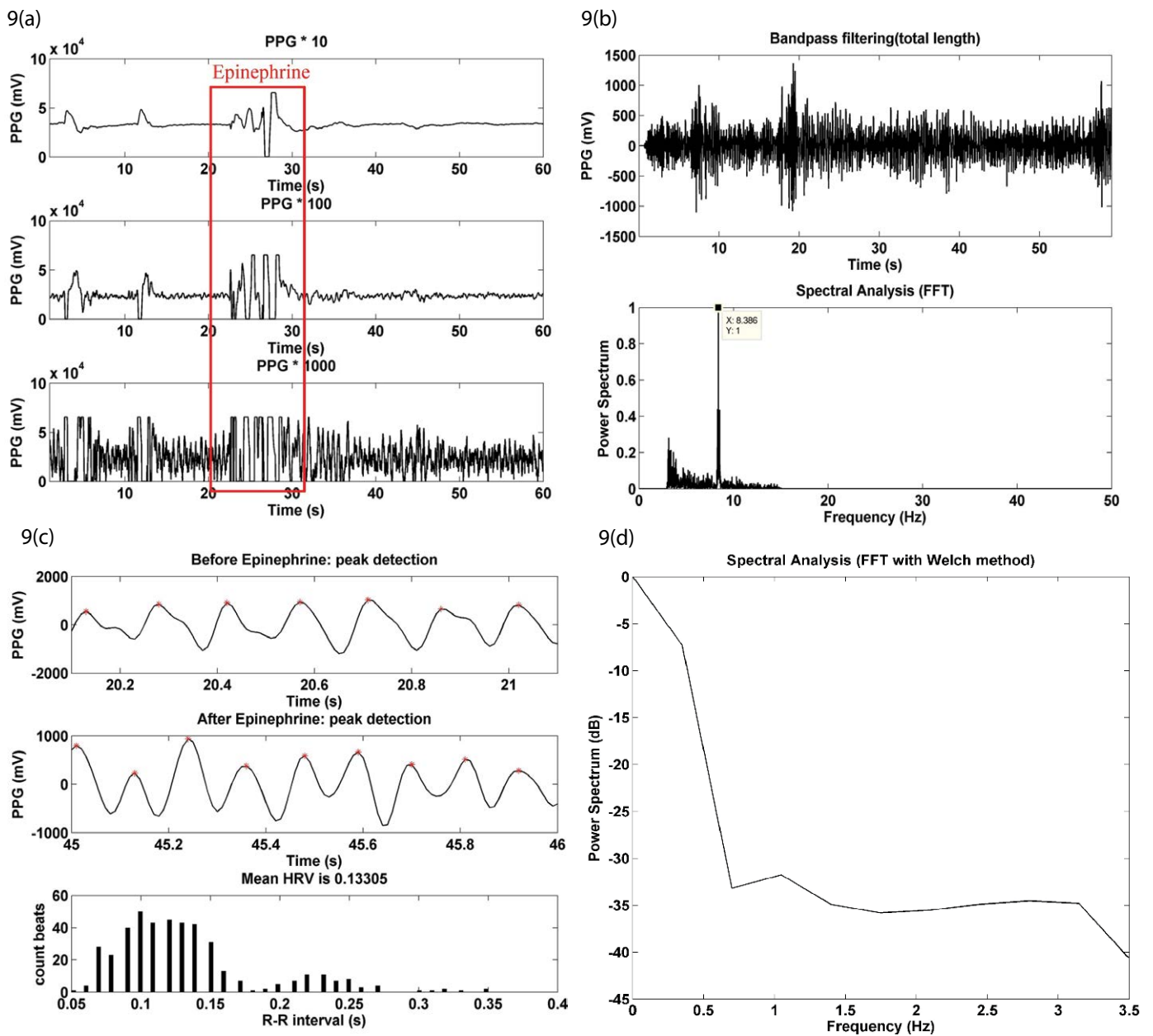


Figure 9: Experimental results before and after the use of epinephrine in the retrained state.

saturated during the injection, as in the previous two cases. As illustrated in **Figure 10(b)**, there was a significant rise in the power spectrum of a bandpass filtered PPG signal below 5 Hz, as an effect of motion artifact. Instead, the heart rate signal of interest was suppressed considerably in this case. As in the previous two cases, there was a distinguishable difference in the peak detection waveforms between before and after the injection of epinephrine **Figure 10(c)**. In comparison with **Figure 7(d)**, there was a slight increase in the HRV spectrum over low frequency components in **Figure 10(d)**.

■ Heart rate measurement in the running state

This presented apparatus aims to remove motion artifact in such a way as to extract the heart rate signal of interest in the running state. Motion artifact can be nothing more than acceptable level of noise, or can cause serious problems such as overriding PPG signals. In this work, raw PPG signals can be sorted into “good” and “poor” signals. In the former case, the desirable heart rate signal can be extracted simply using a bandpass filter and an adaptive filter. In the latter case, introduction of HHT is required for

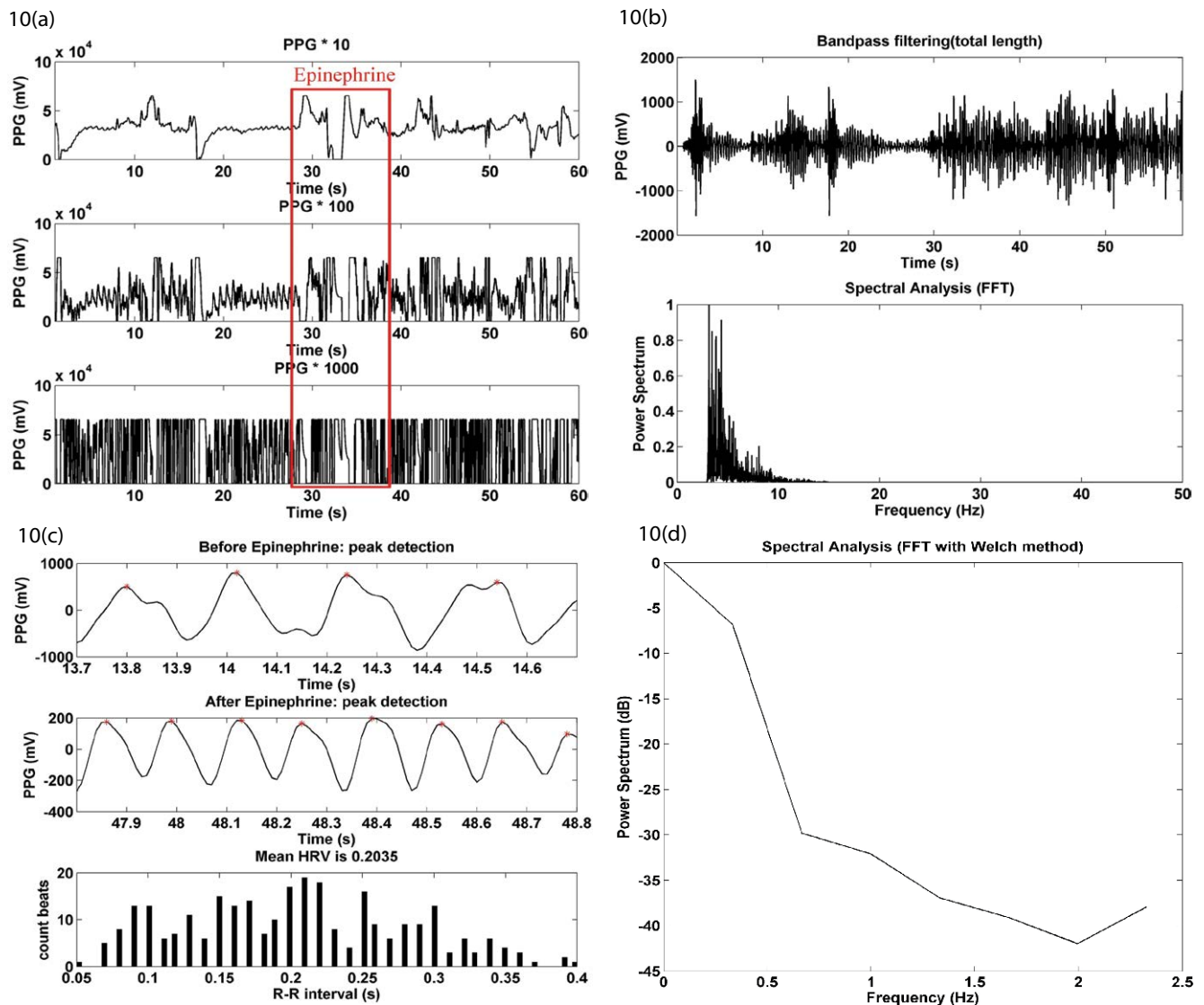


Figure 10: Experimental results before and after the use of epinephrine in the freely moving state.

heart rate signal extraction. These two cases are detailed as follows.

■ **Good signal case**

“Good” signal processing is illustrated with **Figure 11**. The upper half of **Figure 11(a)** gives the acceleration signals along the x, y and z axes of a g-sensor, and, for illustration purposes, the lower half is the amplified PPG signals at respective stages of a cascade amplifier. A close observation on the g-sensor signals reveals that there is a frequency consistency among the g-sensor signals. For the purpose of motion artifact removal, the strongest, but mostly unsaturated, signal is applied to the adaptive filter, illustrated in **Figure 4**, as the input signal $S + n_o$, and a g-sensor signal is as the reference

signal n_i . As illustrated in **Figure 11(b)**, bandpass filtering of the output signal at the second stage clearly indicates two dominant frequencies at 3.03 and 6.7 Hz, respectively. The major 3.03 Hz component is interpreted as an effect of motion artifact, while the minor 6.7 Hz component is presumed as the desired heart rate of a rat, and is completely filtered out subsequently, using the adaptive filter. Hence, it is evident that the 6.7 Hz component is the heart rate signal of interest. **Figure 11(c)** gives the peak detection waveform in the running state, and gives an RRI histogram of the first 100 pieces of data with an average of 0.19. **Figure 11(d)** illustrates the HRV spectrum.

■ **Poor signal case**

“Poor” signal processing is illustrated with **Figure**

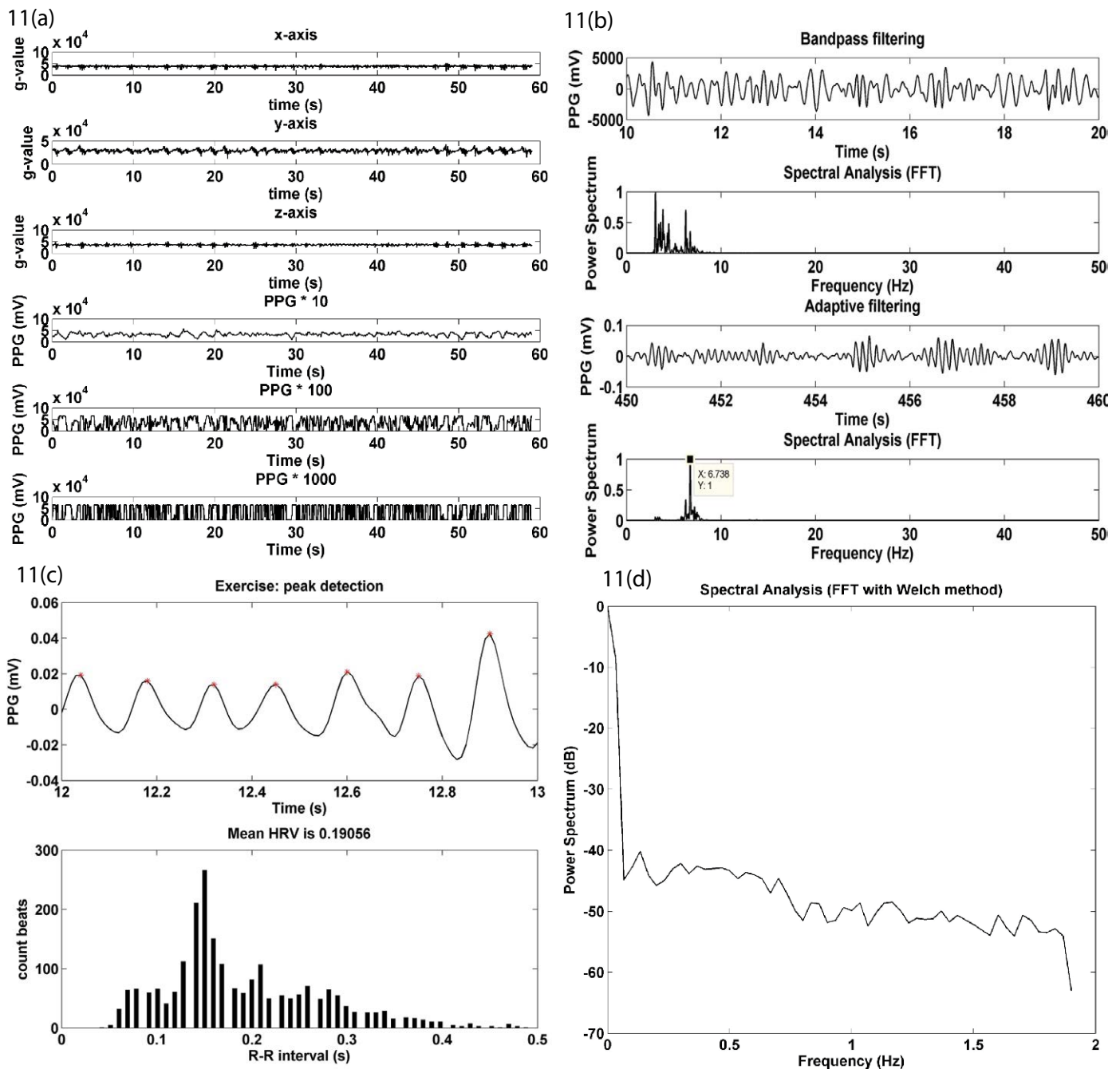


Figure 11: Experimental results in a good signal case in the running state.

12. As in **Figure 12(a)**, the upper half of **Figure 12(a)** gives the acceleration signals along the x, y and z axes of the g-sensor, and, for illustration purposes, the lower half is the amplified PPG signals at respective stages of a cascade amplifier. The output signal saturation was very frequently observed at the second and the third stages. As illustrated in **Figure 12(b)**, a combined use of bandpass and adaptive filtering does not as in **Figure 12(b)** to remove the motion artifact, nor does significantly highlight the

presumed heart rate signal at 7.2 Hz. As can be found in **Figure 12(c)**, HHT now serves as a way to remove the unwanted motion artifact, and further highlight the 7.2 Hz component. **Figure 12(d)** gives a peak detection waveform of **Figure 12(c)**, and then gives an RRI histogram with an average of 0.17.

- Protocol
- Rats under test

Tested adult male Sprague-Dawley rats,

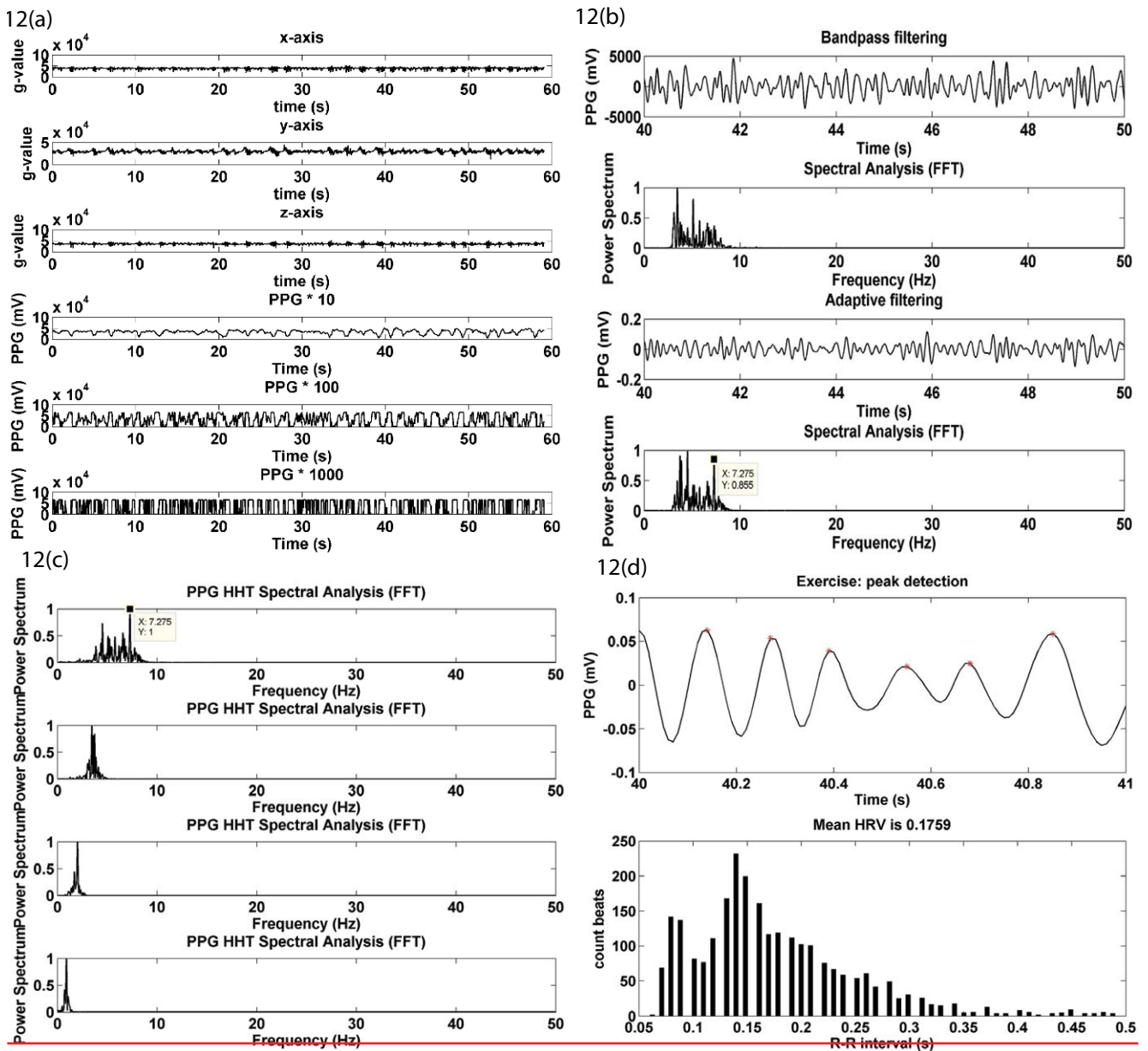


Figure 12: Experimental results in a poor signal case in the running state.

weighing between 270–320 g, were purchased from the National Laboratory Animal Center, Taiwan. Exposed to 12 hours of daylight and darkness per day, they were raised in an air-conditioned room at $24 \pm 1^\circ\text{C}$, and there was no food-water restriction in rats. All the experiments were conducted in day time, and the protocol was approved by the committee on the ethics of animal experiments in Chi Mei Medical Center, Tainan, Taiwan.

■ Middle cerebral artery occlusion (MCAo)

MCAo was induced with the intraluminal filament model by Longa [29]. Rats were anesthetized and maintained with 1–3%

halothane in 70% N₂O and 30% O₂ with a facemask. Then, the left common carotid, internal carotid artery (ICA), and the external carotid artery (ECA) were exposed by a surgical operation. The CCA and ECA portions were then tied with a white thread. A filament (a 4-0 nylon suture with a blunted tip, 0.37 mm in diameter; Doccol Corporation, USA) coated with poly-Llysine was inserted into the right ECA. Next, the direction of the suture was altered toward the ICA and the suture was extended to occlude the MCA. Reperfusion was established by withdrawing the filament under anesthesia at the end of 60 min.

■ Inclined plane test

An inclined plane test is a quantitative measure of a rat's motor function recovery after an ischemic stroke. The test is done by measuring the hind, or rear, limb grip strength of a rat. As presented in [30], the test involved a 60×60 cm acrylic plane with the inclination angle ranging between 0 and 70°. On the inclined plane, there was a rectangular box as a rat house and a rubber ribbed surface at the house exit. Once released from the house with the head downward in this work, a rat reflexly caught the rubber ribbed surface to avoid sliding down using hind limbs. Starting at an angle of 25°, the motorized plane continued to incline until the rat failed to catch the rubber ribbed surface. Then the motor stopped, and the sliding angle was recorded.

■ Protocol

To begin with, rats under test were randomly sorted into the control and the exercise groups, each composed of seven members ($n = 7$). As in [17,18], a 3-week high-intensity physical fitness training program was conducted on all the rat members, five days a week. In week 1, the members were trained for half an hour with a maximum speed of 20 m/minute, in week 2 for an hour with a maximum speed of 20 m/minute, and in week 3 for an hour with a maximum speed of 30 m/minute. In contrast, all the members in the control group did not take part in any training program. As illustrated in **Figure 13**, MCAo was performed on all the members of both groups right after the end of the training program, and a subsequent 7-day behavioral assessment was conducted using an inclined plane test.

Results

■ Heart rate observation over a complete cycle

As illustrated in **Figure 14**, a complete measure cycle for rat runners is made up of 3 phases. Phases 1–3 refer to a 10-minute pre-exercise, a 1-hour exercise and a 10-minute post-exercise duration, respectively. **Figure 14(a)** gives the PPG signals in phase 1, accompanied by motion artifact in the freely moving state. **Figure 14(b)** gives the extracted PPG signal in the running state using an adaptive filter and HHT. Finally, **Figure 14(c)** gives a smooth post-exercise PPG signal in the absence of motion artifact, due to the fact that the rats needed to gasp for air and kept still accordingly.

As illustrated in **Figure 14(d)**, the members of the control group were measured to have an average heart rate between 304 and 324 BPM. The heart rate rose linearly with time until 500 BPM was reached approximately at 5 minutes after the start of phase 2. Ever since, the heart rate was well maintained during phase 2 with an average of 487 BPM, and fell to 400–410 BPM at 3 minutes after the start of phase 3. It is noted that the average heart rate was measured as 405 BPM approximately at the end of phase 3, meaning that it took the rat runners longer than 10 minutes to recover the heart beat to its initial condition.

■ Heart rate comparison between groups

Figure 15 gives a heart rate comparison between both groups during the 3-week physical training program. A 10-min PPG signal measurement was performed on the members of the control group at the same time each day, while was repeated on the exercise group during the pre-exercise phase for comparison purposes. As illustrated, the control group has an average heart rate of 356.89 BPM, while the exercise group has 358.31 BPM in week 1; 360.1 BPM, 328.21 BPM in week 2; 361.68 BPM, 312.91 BPM in week 3. A significant difference in the average heart rate is clearly seen between both groups in weeks 2 and 3, and is interpreted as a benefit of daily workout.

■ Correlation between heart rate and inclination angle

In the 7-day behavioral assessment, inclined plane tests gave an inclination angle of 53 ± 0.39 degrees in the exercise group, and 43 ± 0.73 degrees in the control group, as a way to demonstrate a benefit of exercise preconditioning. With the measured inclination angles superimposed over the week 3 result of **Figure 15** for comparison purposes, it is clearly seen in **Figure 16** that there exists a negative correlation between the heart rate and the inclination angle, meaning that the heart rate can be viewed for sure as a measure of exercise preconditioning.

Discussion

This paper aims to develop a non-invasive apparatus for physiological signal measurement. PPG signals, accompanied by motion artifact, were sensed using a front-end sensor array attached to the tail of a rat under test, and desired PPG signal was extracted in the back end using an adaptive filter and HHT. The performance of this

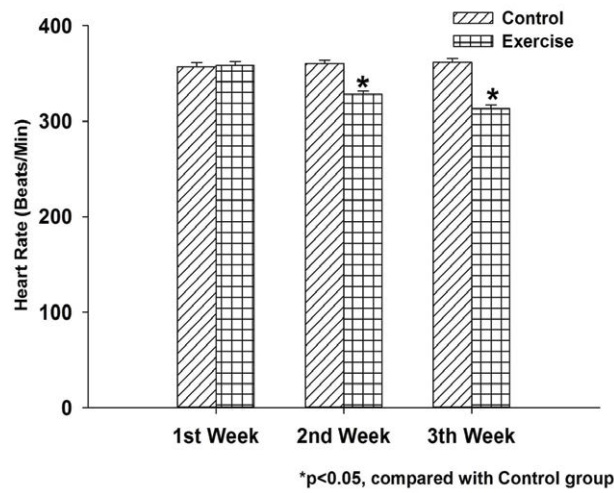


Figure 15: Average heart rate comparison between the control and the exercise groups for weeks 1–3.

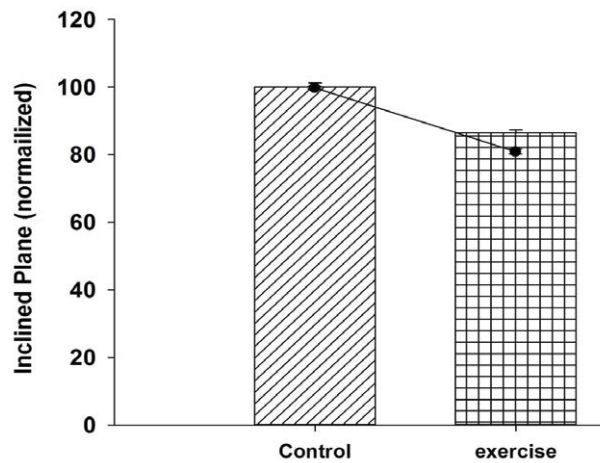


Figure 16: Correlation between the average heart rate and the result of an inclined plane test in week 3.

vessels, meaning that there is no alignment problem between the front-end sensor array and a measurement spot. In simple terms, PPG signals can be sensed anywhere along the tail, not as in [23], where there is a need to precisely attach a ECG sensor to a specific spot on the chest of a rat. For this sake, the physical confinement problem, experienced particularly in the running state, can be resolved not fully, but to a great extent. As many know, PPG signals are susceptible to motion artifact. A way is presented herein to effectively remove the motion artifact, and the heart rate signal of interest can be extracted consequently via the best of nine PPG waveforms in terms of unsaturated signal amplification. A combined use of the presented measurement apparatus and an IR sensor-equipped running wheel, as

proposed in [17], is expected to outperform the other testbeds in terms of signal stability, particularly in the running state. This is simply due to the fact that the IR sensor-equipped running wheel is designed to have an adaptive acceleration-training model to prevent rats under test from falling during a training program. Short of this training model, signal instability inevitably occurs when rats were trained using all the commercial treadmills and running wheels. Hence, this work stands as a superior testbed for physiological condition monitoring due to the use of well-measured raw PPG signal and a well-perform signal extraction.

Up to now, wireless physiological animal experiments are mostly conducted using invasive measurement systems. A major problem is the risk of surgery and the signal quality

due to the way signals are acquired. **Table 1** gives a comparison in many aspects among this work and representative pieces of prior art [19,23,25], which are an invasive, a non-invasive, but location-dependent and a non-invasive, measurement apparatus, respectively. As clearly indicated therein, this work offers an advantageous way to measure PPG signals in terms of the physical confinement imposed on rats, the cost and the difficulty attaching sensors, an integration with a training model, and more.

Physiological response to exercise stress testing has long been an issue of great interest to medical research scientists [31-33], while experimental results remain questioned since animals already got hurt to a certain extent after electrodes implantation surgery. For this sake, a wearable, low physical confinement, non-invasive physiological measurement apparatus was designed, integrated with a high-performance running wheel-based physical training mechanism, and expected to provide more convincing results. The exercise, but not the control, group members took a 3-week physical training program for heart rate comparison. Following well-performed signal extraction, it is indicated that the exercise group demonstrated a much lower average heart rate than the control group during the pre-exercise stage of week 2. The average heart rate was well maintained at 500 BPM approximately during the exercise stage, and went downward to somewhere between 400 and 450 BPM during the post-exercise stage, meaning that a 10-minute rest is not long

enough to resume the initial state of heart rate. Following the 3-week physical training program, MCAo operation was performed on all the rat members in both groups, and motion function impairment was assessed using an inclined plane test. The exercise group members were found to have a lower average heart rate than the control group, a presumed advantage of exercise preconditioning. More importantly, there exists a negative correlation between the heart rate and the inclination angle of the test, evidence that the heart rate can be viewed as a measure of exercise benefit.

Thus far, there remains much room for the development of animal physiological monitoring systems as an effective stroke prevention mechanism. For this sake, a running wheel-based, and IR sensor-equipped, test bed was developed herein for monitoring on rats under test using a well-performed signal extraction. As an extension and an ultimate goal of this work, an objective, effective and particularly adaptive physiological monitoring test bed is scheduled to be developed by our team in the very near future for human stroke prevention.

Conclusion

This paper presents an IR sensor-equipped, running wheel-based rat test bed whereby non-invasive, physiological monitoring is performed on rats in four states, meaning that surgical risk in a conventional invasive measurement can be completely removed. Not as in existing wearable

Table 1: Performance and requirement comparison among this work and representative pieces of prior art.

Features	Invasive [19]	Non-invasive, location-dependent [25]	Non-invasive [23]	Non-invasive, location-independent (this proposal)
Physiological state of animals under test	Anesthetized, restrained, freely moving, running	Anesthetized, restrained	Anesthetized, restrained	Anesthetized, restrained, freely moving, running
Exercise monitoring	Available	Not available	Not available	Available
Level of physical confinement	No	No	High	Low
Complexity of sensor attachment	High (a sensor implant surgery was required)	Low (animals were directly placed on a test bed)	Intermediate (a tight body-worn sensor was a necessity)	Low (a tail-worn sensor is required)
Rat size	Large, Medium	Large, Medium, Small	Large, Medium, Small	Large, Medium, Small
Integration into an animal test bed	Not available	Not available	Not available	Available
Measure of effective exercise	Not available	Not available	Not available	Available
Dynamic physiological monitoring	Available	Not available	Not available	Available
Long-term, continuous physiological monitoring	Not available	Available	Available	Available
Cost	High	Low	Low	Low

devices, the aim of low physical confinement can be reached by attaching PPG sensors to the tail root of a rat. The heart rate signal of interest can be successfully extracted out of raw PPG signal using an adaptive filter and HHT. All the rat members in the exercise group took a 3-week physical training program for a heart rate observation over a complete cycle, consisting of a pre-exercise stage, an exercise stage and a post-exercise stage. The exercise group members were found to have a much slower average heart rate than the control group in weeks 2 and 3. More importantly, the heart rate observation in week 3 clearly indicated a negative correlation with a quantitative measure, i.e. the result of an inclined plane test. In simple terms, the heart rate was experimentally validated herein as a non-invasive alternative to an inclined plane test for the assessment of physical impairment due to stroke. The benefit of exercise to disease prevention remains an issue of great interest in neurological physiology, while researchers have a difficulty monitoring the physiological conditions of animals in real time. For this sake, this paper presents a

well-designed rat test bed as a solution to the above-stated problem for physiologists.

Acknowledgment

The authors would like to thank Dr. Jhi-Joung Wang, who is the Vice Superintendent of Education at Chi-Mei Medical Center, and Dr. Chih-Chan Lin from the Laboratory Animal Center, Department of Medical Research, Chi-Mei Medical Center, 901 Zhonghua, Yongkang Dist., Tainan City 701, Taiwan, for providing the experimental environment. They would also like to thank Miss Ling-Yu Tang from the Department of Medical Research, Chi-Mei Medical Center, Tainan, Taiwan, for their valuable assistance in real experiments with rats.

Funding

The author gratefully acknowledges the support provided for this study by the Ministry of Science and Technology (MOST 106-2221-E-167 -004 -MY3) of Taiwan.

References

- Wilson B, Forrester S, Kawata K, et al. Effects of voluntary exercise preconditioning on ang ii-induced cardiovascular pathophysiology in the mouse. *Faseb. J* 29(1), (2015).
- Xu T, Tang H, Zhang B, et al. Exercise preconditioning attenuates pressure overload-induced pathological cardiac hypertrophy. *Int. J. Clin. Exp. Pathol* 8(1), 530-540 (2015).
- Liebelt B, Papapetrou P, Ali A, et al. Exercise preconditioning reduces neuronal apoptosis in stroke by up-regulating heat shock protein-70 (heat shock protein-72) and extracellular-signal-regulated-kinase 1/2. *Neuroscience* 166(1), 1091-1100 (2010).
- Zhang F, Wu Y, Jia J. Exercise preconditioning and brain ischemic tolerance. *Neuroscience* 177(1), 170-176 (2011).
- Edouard P. Exercise associated muscle cramps: Discussion on causes, prevention and treatment. *Sci. Sports* 29(1), 299-305 (2014).
- Whittaker JL, Woodhouse LJ, Nettel-Aguirre A, et al. Outcomes associated with early post-traumatic osteoarthritis and other negative health consequences 3-10 years following knee joint injury in youth sport. *Osteoarthritis. Cartilage* 23(1), 1122-1129 (2015).
- Furman J. When exercise causes exertional rhabdomyolysis. *JAAPA* 28(1), 38-43 (2015).
- McKenna MC, Lavin P. High-intensity exercise in a young man resulting in rhabdomyolysis with acute kidney injury. *Ir. J. Med. Sci* 184(1), 312-313 (2015).
- Patel DP, Redshaw JD, Breyer BN, et al. High-grade renal injuries are often isolated in sports-related trauma. *Injury* 46(1), 1245-1249 (2015).
- Santos-Lozano A, Sanchis-Gomar F, Garatachea N, et al. Incidence of sudden cardiac death in professional cycling: Sudden cardiac death and exercise. *Int. J. Cardiol* 223(1), 222-223 (2016).
- Ding Y, Li J, Luan X, et al. Exercise preconditioning reduces brain damage in ischemic rats that may be associated with regional angiogenesis and cellular overexpression of neurotrophin. *Neuroscience* 124(1), 583-591 (2004).
- Jin J, Kang H-M, Park C. Voluntary exercise enhances survival and migration of neural progenitor cells after intracerebral haemorrhage in mice. *Brain. Inj* 24(1), 533-540 (2010).
- Liebetanz D, Gerber J, Schiffner C, et al. Pre-infection physical exercise decreases mortality and stimulates neurogenesis in bacterial meningitis. *J. Neuroinflammation* 9(1), 168 (2012).
- Wang RY, Yang YR, Yu SM. Protective effects of treadmill training on infarction in rats. *Brain. Res* 922(1), 140-143 (2001).
- Li J, Luan XD, Clark JC, et al. Neuroprotection against transient cerebral ischemia by exercise pre-conditioning in rats. *Neurol. Res* 26(1), 404-408 (2004).
- Chen CC, Chang MW, Chang CP, et al. A forced running wheel system with a microcontroller that provides high-intensity exercise training in an animal ischemic stroke model. *Braz. J. Med. Biol. Res* 47(1), 858-868 (2014).
- Chen CC, Chang MW, Chang CP, et al. Improved infrared-sensing running wheel systems with an effective exercise activity indicator. *PLoS. One* 10(1), e0122394 (2015).
- Leasure JL, Jones M. Forced and voluntary exercise differentially affect brain and behavior. *Neuroscience* 156(1), 456-465 (2008).
- Fu X, Chen W, Ye S, et al. A wireless implantable sensor network system for in vivo monitoring of physiological signals. *IEEE. Trans. Inf. Technol. Biomed* 15(1), 577-584 (2011).
- Miller LE, Hosick PA, Wrieden J, et al. Evaluation of arrhythmia scoring systems and exercise-induced cardioprotection. *Med. Sci. Sports. Exerc* 44(1), 435-441 (2012).
- Quindry JC, Miller L, McGinnis G, et al. Ischemia reperfusion injury, K-ATP channels, and exercise-induced cardioprotection against apoptosis. *J. Appl. Physiol* 113(1), 498-506 (2012).
- Schierok H, Markert M, Pairet M, et al. Continuous assessment of multiple vital physiological functions in conscious freely moving rats using telemetry and a

- plethysmography system. *J. Pharmacol. Toxicol. Methods* 43(1), 211-217 (2000).
23. Pereira-Junior PP, Marocolo M, Rodrigues FP, et al. Noninvasive method for electrocardiogram recording in conscious rats: feasibility for heart rate variability analysis. *An. Acad. Bras. Cienc* 82(1), 431-437 (2010).
24. Mongue-Din H, Salmon A, Fiszman MY, et al. Non-invasive restrained ECG recording in conscious small rodents: a new tool for cardiac electrical activity investigation. *Pflugers. Arch* 454(1), 165-171 (2007).
25. Sato S, Yamada K, Inagaki N. System for simultaneously monitoring heart and breathing rate in mice using a piezoelectric transducer. *Med. Biol. Eng. Comput* 44(1), 353-362 (2006).
26. Huang NE, Shen Z, Long SR, et al. The empirical mode decomposition and the Hilbert spectrum for nonlinear and non-stationary time series analysis. *Proc. R. Soc. A* 454(1), 903-995 (1998).
27. Li H, Kwong S, Yang L, et al. Hilbert-Huang transform for analysis of heart rate variability in cardiac health. *IEEE/ACM. Trans. Comput. Biol. Bioinform* 8(1), 1557-1567 (2011).
28. Choi Y, Zhang Q, Ko S. Noninvasive cuffless blood pressure estimation using pulse transit time and Hilbert-Huang transform. *Comput. Electr. Eng* 39(1), 103-111 (2013).
29. Longa EZ, Weinstein PR, Carlson S, et al. Reversible middle cerebral artery occlusion without craniectomy in rats. *Stroke* 20(1), 84-91 (1989).
30. Chang MW, Young MS, Lin MT. An inclined plane system with microcontroller to determine limb motor function of laboratory animals. *J. Neurosci. Methods* 168(1), 186-194 (2008).
31. Madias JE, Agarwal H. Unusual ECG responses to exercise stress testing. *J. Electrocardiol* 34(1), 265-269 (2001).
32. Verrier RL, Malik M. Clinical applications of T-wave alternans assessed during exercise stress testing and ambulatory ECG monitoring. *J. Electrocardiol* 46(1), 585-590 (2013).
33. Altini M, Casale P, Penders J, et al. Personalized cardiorespiratory fitness and energy expenditure estimation using hierarchical Bayesian models. *J. Biomed. Inform.* 56(1), 195-204 (2015).